



HBr or not HBr? That is the question: crystal structure of 6-hydroxy-1,4-diazepane-1,4-dium dibromide redetermined

Mateusz Piontek,^a Bernd Morgenstern,^a Nils Steinbrück,^b Bastian Oberhausen,^b Guido Kickelbick^b and Kaspar Hegetschweiler^{a*}

Received 25 March 2019

Accepted 17 April 2019

Edited by M. Kubicki, Adam Mickiewicz University, Poland

Keywords: dihydrobromide; crystal structure; protonated diamine; misinterpreted H atom; series-termination error.

CCDC reference: 1910784

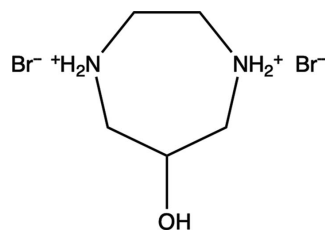
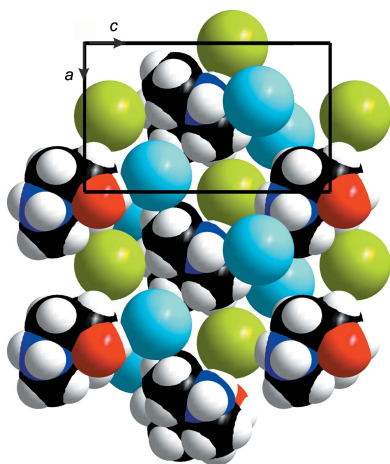
Supporting information: this article has supporting information at journals.iucr.org/c

^aInorganic Chemistry, Universität des Saarlandes, Campus C4.1, 66123 Saarbrücken, Germany, and ^bInorganic Solid State Chemistry, Universität des Saarlandes, Campus C4.1, 66123 Saarbrücken, Germany. *Correspondence e-mail: hegetschweiler@mx.uni-saarland.de

Liu *et al.* [*Chin. J. Struct. Chem.* (1996), **15**, 371–373] reported the structure of 6-hydroxy-1,4-diazepane di(hydrogen bromide), C₅H₁₂N₂O·2HBr, which was interpreted in terms of neutral diazepane and HBr molecules. We found, however, ample evidence that the formation of an organic salt, consisting of a diammonium cation and two bromide anions, is more plausible. This interpretation is also in agreement with thermogravimetric analysis and with the observed solution behaviour. The crystal structure of 6-hydroxy-1,4-diazepane-1,4-dium dibromide, C₅H₁₄N₂O²⁺·2Br⁻, measured at 142 K, crystallized in the orthorhombic space group *P*2₁2₁2₁. The structure displays O—H···Br and N—H···Br hydrogen bonding. Contact distances are given. A search in the Cambridge Structural Database for the singly-bonded H—Br moiety revealed a total of 69 structures. The question, whether these structures really include HBr as neutral molecules or rather Br⁻ anions and a protonated substrate such as an amine, is addressed.

1. Introduction

6-Hydroxy-1,4-diazepane (dazol) was first synthesized by Saari *et al.* (1971) and has been used as a tridentate facially coordinating metal-complexing agent (Liu *et al.*, 1997a). The free ligand has been isolated as a dihydrogen bromide, C₅H₁₂N₂O·2HBr, and its crystal structure has been reported [Liu *et al.*, 1996; Cambridge Structural Database (CSD; Groom *et al.*, 2016) refcode TOKTIW]. The authors postulated crystallization of the neutral diazepane as a free base together with two HBr molecules. From a chemical point of view, the formation of discrete HBr molecules beside a basic entity is surprising, even taking into account that the situation in the solid state does not necessarily reflect the well-known acid–base properties in aqueous solution. However, a search for molecular H—Br in the CSD (Version 5.20, 2018) gave a total of 69 hits and hence some support for the molecular



model. To shed light on this discrepancy, we have: (i) investigated the chemistry of dazol in aqueous solution using potentiometric titration experiments and pD-dependent ¹H

NMR spectroscopy, and (ii) prepared a crystalline sample of the title compound (see Scheme), repeated the structure determination reported by Liu *et al.* (1996) and performed additional thermogravimetric measurements to elucidate the solid-state properties.

2. Experimental

2.1. Synthesis and crystallization

The synthesis of the title compound was performed following the protocol given by Saari *et al.* (1971) with minor modifications. *N,N'*-Dazolbis(toluenesulfonamide) was prepared as described by the reaction of *N,N'*-ethylenebis(toluenesulfonamide) with 2,3-dibromopropan-1-ol. However, in the next step, the detour *via* the acetate proved not necessary. The two toluenesulfonamide groups could be removed directly without any loss of yield by heating the bis(toluenesulfonamide) suspended in 48% aqueous HBr to 125 °C for 3 h. The clear bright-yellow solution was allowed to cool to room temperature and was then evaporated to dryness under reduced pressure. The resulting solid was washed with diethyl ether and ethanol to yield the title compound as a pale-gray solid (91%). Crystals were grown by slow diffusion of EtOH into an aqueous solution of the product which has been acidified with additional HBr.

2.2. Refinement

Liu *et al.* (1996) reported an unambiguous location of the C-, N-, O- and Br-atom positions of one dazol moiety and two crystallographically independent Br atoms. It is clear that a reliable assignment of H-atom positions is more difficult, and might even be a highly questionable task, if the high electron density of the two heavy Br atoms is considered. Unfortunately, the data set of Liu *et al.* (1996) is of rather poor quality. According to the CSD, the data set was recorded at room temperature. Moreover, the information provided by these authors is not really conclusive. In their Table 1 (and in the CIF available from the CSD), the H-atom positions are all listed without standard deviations and the authors stated that 'H atoms were located by geometric method except the hydroxyl one, which was oriented from difference Fourier map.' This statement seemingly indicates that the H(–Br), H(–C) and H(–N) positions have not been taken from a difference Fourier map. It is confusing that some of the C–H (1.13 Å) and N–H (1.15 Å) distances and H–C–H (93.2°) angles do not fall in expected ranges. Obviously, the authors did not apply the usual riding model with fixed angles and distances. The two H–Br lengths of 1.04 and 1.08 Å are also rather short.

To improve the quality of the data set, we performed a data collection at –131 °C. The space group and lattice parameters, as well as the positional parameters of the non-H atoms, were all in agreement with Liu's report (Liu *et al.*, 1996). Crystal data, data collection and structure refinement details are summarized in Table 1. Inspection of a difference Fourier map unambiguously yielded all of the H(–C) and H(–O)

Table 1
Experimental details.

Crystal data	
Chemical formula	C ₅ H ₁₄ N ₂ O ²⁺ ·2Br [–]
<i>M_r</i>	278.00
Crystal system, space group	Orthorhombic, <i>P</i> 2 ₁ 2 ₁ 2 ₁
Temperature (K/°C)	142/–131
<i>a</i> , <i>b</i> , <i>c</i> (Å)	7.7005 (4), 9.2774 (5), 12.6853 (6)
<i>V</i> (Å ³)	906.25 (8)
<i>Z</i>	4
Radiation type	Mo <i>K</i> α
<i>μ</i> (mm ^{–1})	8.89
Crystal size (mm)	0.23 × 0.07 × 0.02
Data collection	
Diffractometer	Bruker APEXII CCD
Absorption correction	Multi-scan (<i>SADABS</i> ; Krause <i>et al.</i> , 2015)
<i>T_{min}</i> , <i>T_{max}</i>	0.576, 0.746
No. of measured, independent and observed [<i>I</i> > 2σ(<i>I</i>)] reflections	4858, 2089, 1789
<i>R_{int}</i>	0.050
(sin θ/λ) _{max} (Å ^{–1})	0.652
Refinement	
<i>R</i> [<i>F</i> ² > 2σ(<i>F</i> ²)], <i>wR</i> (<i>F</i> ²), <i>S</i>	0.037, 0.063, 0.93
No. of reflections	2089
No. of parameters	106
No. of restraints	5
H-atom treatment	H atoms treated by a mixture of independent and constrained refinement
Δρ _{max} , Δρ _{min} (e Å ^{–3})	0.61, –0.51
Absolute structure	Flack <i>x</i> determined using 646 quotients [(<i>I</i> ⁺) – (<i>I</i> [–])] / [(<i>I</i> ⁺) + (<i>I</i> [–])] (Parsons <i>et al.</i> , 2013)
Absolute structure parameter	0.05 (2)

Computer programs: *APEX2* (Bruker, 2010), *SAINTE* (Bruker, 2010), *SHELXT2014* (Sheldrick, 2015a), *SHELXL2014* (Sheldrick, 2015b), *DIAMOND* (Brandenburg, 2007) and *PLATON* (Spek, 2009).

hydrogens with meaningful bond lengths and angles. The positional parameters of these H atoms were now included in a subsequent refinement using a riding model, with an appropriate restraint for H(–O) and appropriate constraints for the H(–C) atoms. At this stage, the refinement provided agreement factors of *R*₁ = 3.94% and *wR*₂ = 7.47%. The two most intense peaks, with electron densities of 0.72 and 0.70 e Å^{–3}, in the new difference Fourier map were located in proximity to atoms N2 and N1, respectively. They were interpreted as H(–N) positions. Further refinement confirmed this assignment and gave a slight drop of the *R*₁ (3.85%) and *wR*₂ (6.64%) values. A subsequent difference Fourier map exhibited more than 30 unassigned peaks with electron densities in the range 0.62–0.42 e Å^{–3}. The four peaks with highest intensities (*Q*₁–*Q*₄) were located in proximity to atoms N1, Br2, N2 and Br1 (in this order). At this stage, two different models were considered for the final refinement. Model *A* comprised *Q*₁ and *Q*₃, which were both interpreted as H(–N) positions; *Q*₂ and *Q*₄ were disregarded. Model *B* comprised *Q*₂ and *Q*₄ as H(–Br) positions, with *Q*₁ and *Q*₃ now being neglected. Free refinement of model *A* resulted in a stable and meaningful result, yielding two NH₂⁺ groups, whereas the free refinement of model *B* collapsed: the H(–Br) atoms moved to positions with very short Br–H distances (<0.3 Å). The agreement factors of model *A* (*R*₁ =

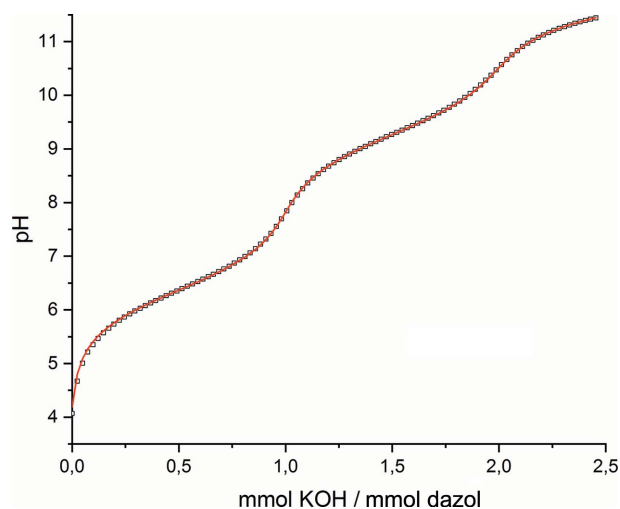


Figure 1
Titration curve (25 °C, 0.1 M KCl) of $\text{H}_2\text{dazol}^{2+}$. Squares refer to the measured values. The red line was calculated using the deprotonation constants $-\log K_{a,1} = 6.01$ and $-\log K_{a,2} = 9.05$.

3.72% and $wR_2 = 6.31\%$) were marginally better than those of model *B* ($R_1 = 3.84\%$ and $wR_2 = 6.63\%$). These results clearly show that the crystal structure analysis alone does not allow discrimination with certainty between the two models. However, the stable refinement of model *A* and the slightly better agreement factors may be regarded as a first sign for the ionic structure. The observed electron density in proximity to

the Br atoms (*Q2* and *Q4*) could be understood as well-known series-termination errors in the Fourier synthesis (Glusker *et al.*, 1994).

In the final refinement (model *A*), a riding model was used for the C-bonded H atoms. As suggested by Müller *et al.* (2006), the positional parameters of the O- and N-bonded H atoms were refined using isotropic displacement parameters, which were set at $1.5U_{\text{eq}}(\text{O})$ or $1.2U_{\text{eq}}(\text{N})$ of the pivot atom. In addition, restraints of 0.84 and 0.88 Å were used for the O–H and N–H distances, respectively.

3. Results and discussion

3.1. Chemical context

Liu *et al.* (1996) postulated the presence of neutral diazepane as a free base, together with two molecular HBr units in the solid-state structure. At first glance, such an interpretation is amazing, since HBr is known to react as a very strong acid, and the diazepane moiety – as an alicyclic diamine – is expected to react as a base. We investigated the protonation behaviour of dazol in aqueous solution (25 °C) and found – as expected – that an uptake of two protons occurred readily upon addition of acid. A series of potentiometric titration experiments (Fig. 1) revealed two pK_a values of 6.01 and 9.05 (0.1 M KCl) or 6.37 and 9.28 (1 M KNO_3) for $\text{H}_2\text{dazol}^{2+}$. These values are in agreement with those reported for related amino alcohols (Martincigh & Marsicano, 1995). In addition, we also performed a ^1H NMR titration experiment in D_2O (Fig. 2) and

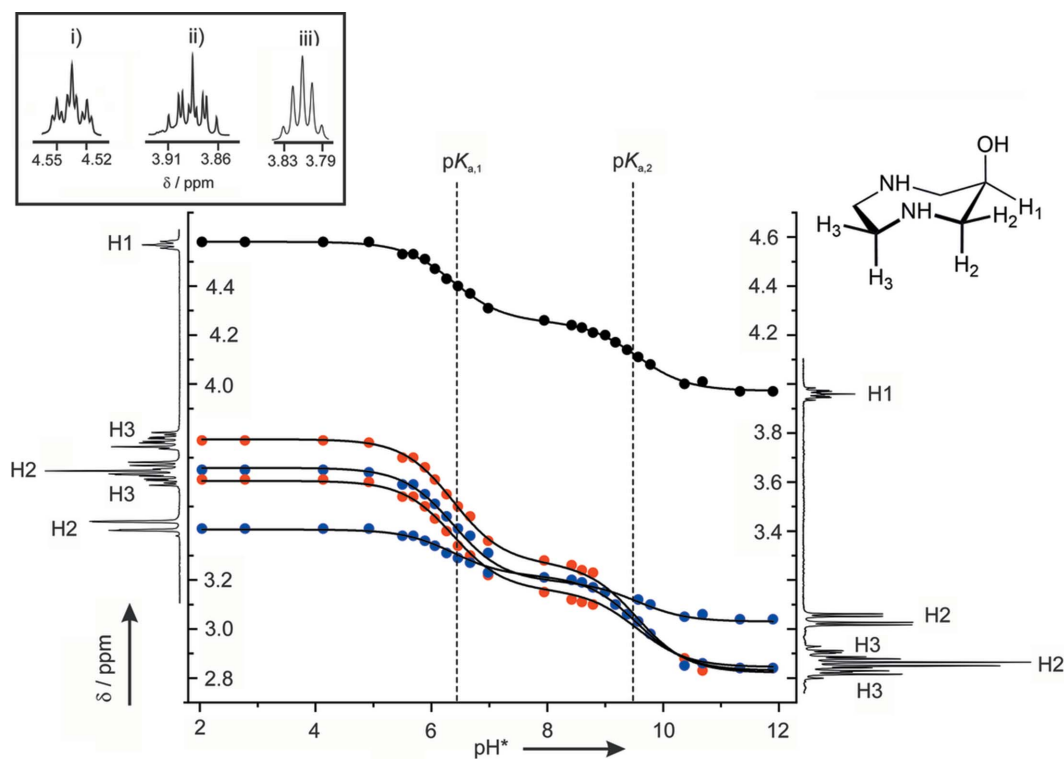


Figure 2
 pH^* dependence of the various ^1H resonances for the nonlabile protons (pH^* refers to the uncorrected pH-meter reading in D_2O for an electrode calibrated in H_2O). The observed resonances (δ_{obs}) are shown as closed circles: H1 (black), H2 (blue) and H3 (red). The lines were calculated [minimization of $\Sigma(\delta_{\text{obs}} - \delta_{\text{calc}})^2$]. Inset: The pattern of H1 at (i) $\text{pH}^* = 5$, (ii) $\text{pH}^* = 10$ and (iii) in $5 \text{ mol l}^{-1} \text{NaOD}$.

observed characteristic pD-dependent resonances for the H(–C) protons upon addition of NaOD. This pD dependency could again be interpreted as a twofold deprotonation reaction of the dication. The evaluated pK_a values in this medium are 6.35 and 9.62. All these characteristics clearly indicate that addition of two equivalents of HBr to an aqueous solution of dazol results in a complete transformation into the H_2dazol^{2+} dication. Crystal growth of the title compound has indeed been performed in such an acidic aqueous medium. However, one must of course be aware that – in general – the solid state does not necessarily depict the equilibrium composition in solution.

A solid sample of the title compound was therefore investigated by IR spectroscopy, looking at around 2600 cm^{-1} for any H–Br stretch vibration. However, these measurements were not conclusive, since a possible H–Br peak was covered by the intense and broad absorption between 2200 and 3500 cm^{-1} , caused by the various associated N–H and O–H stretching vibrations. Thermogravimetric measurements combined with an IR analysis of the gaseous products was more instructive (Fig. 3). A 20 mg sample was heated by a rate of $10\text{ }^\circ\text{C min}^{-1}$ from room temperature up to $800\text{ }^\circ\text{C}$ and exposed to a steady stream of N_2 (20 ml min^{-1}). Complete degradation occurred almost quantitatively ($>90\%$) in one single step in

the range $300\text{--}400\text{ }^\circ\text{C}$. Evolution of HBr could readily be recognized in the IR spectrum ($2400\text{--}2700\text{ cm}^{-1}$) by its characteristic pattern for the two isotopomers with resolved transitions for the various rotamers (NIST, 2019). In addition, an organic component (O–H, N–H and C–H, and possibly C–C and C–O stretching vibrations, but no CO_2) was formed. These findings are in agreement with a predominant sublimation of the product. It is well known that NH_4Br and its organic derivatives, such as methylammonium bromide sublimate in the range $300\text{--}400\text{ }^\circ\text{C}$ (Ivanov *et al.*, 2019). The remaining small nonvolatile residue ($5\text{--}10\%$) probably indicates some minor decomposition during the sublimation process (formation of elemental carbon, as indicated by a black coating inside the crucible). If a 1:1 stream of N_2 and O_2 (each 20 ml min^{-1}) is applied to the sample during heating, the degradation occurred in more than one step. Again, less than 1% weight loss was noted below $200\text{ }^\circ\text{C}$. Up to $250\text{ }^\circ\text{C}$, the sample weight decreased slightly by about 3%. A first significant step of decomposition was then observed in the range of about $250\text{--}330\text{ }^\circ\text{C}$, with a corresponding weight drop of 21%. This value is clearly smaller than the 29% required for a dissociation of one HBr molecule. The final part of the decomposition reaction occurred in two steps at $350\text{--}400$ ($\sim 50\%$) and $400\text{--}550\text{ }^\circ\text{C}$ ($\sim 22\%$). The IR spectra of the

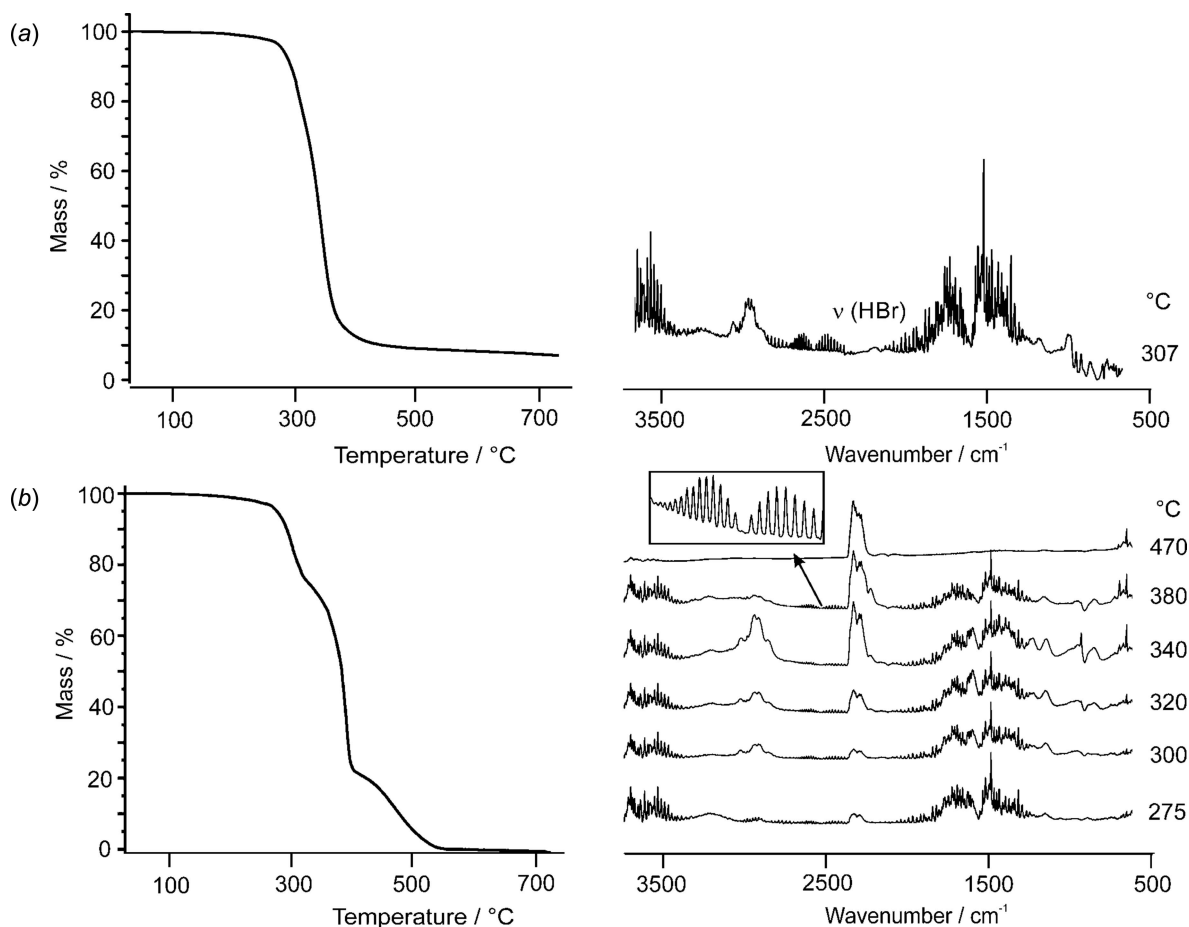


Figure 3 Thermogravimetric analyses of $H_2dazolBr_2$ (%weight versus T) together with IR characteristics of the evolving gases at temperatures as indicated. Heating of the sample (a) in a steady stream of N_2 only and (b) in a 1:1 mixture of N_2 and O_2 . The inset in (b) shows an enlargement for the range $2400\text{--}2700\text{ cm}^{-1}$, indicating the formation of HBr in small traces.

evolving gases showed the formation of H₂O during the entire decomposition reaction. At elevated temperatures (>300 °C), increasing formation of CO₂ and of some organic components (observation of C–H stretching vibrations) was also noted. Above 450 °C, CO₂ remained as the most significant decomposition product. Inspection of the spectra did again exhibit that small traces of HBr have been formed. Maximum HBr production was found around 350–400 °C. These observations do not indicate a simple and quantitative loss of HBr at low temperature. It rather appears that small amounts of HBr are formed *in situ* during the entire decomposition process, particularly at elevated temperatures. As a conclusion, evolution of HBr appears generally to be combined with a complete breakdown of the entire structure.

3.2. Structural commentary

Eliei *et al.* (1965) proposed high conformational flexibility for cycloheptane, with a twist–chair (TC) conformation being of lowest energy. We previously studied 6-amino-1,4-diazepane (daza) as a metal-complexing agent, and the adoption of such a TC conformation for the seven-membered 1,4-diazepane ring of H₃daza³⁺ could indeed be confirmed by crystal structure analysis (Romba *et al.*, 2006; Neis *et al.*, 2010). Its ¹H NMR spectrum exhibited a total of five resonances for the H(–C) protons, indicating a rapid interconversion of different conformations, yielding an averaged structure of higher symmetry (Longuet-Higgins, 2002). The molecular structure of daza and dazol is closely related and similar ¹H NMR characteristics have also been observed for dazol. The coupling pattern of the H(–C–X) proton (H₃daza³⁺: X = NH₃⁺; H₂dazol²⁺: X = OH) revealed, however, some characteristic differences for the two compounds. For H₃daza³⁺, this signal appeared as a triplet of triplets with one large coupling constant of 10.5 Hz and a second much smaller constant of 3.1 Hz. The large coupling of 10.5 Hz is indicative of a staggered orientation of the H–C–C(NH₃⁺)–H fragment, with a torsion angle close to 180°. Obviously, the primary ammonium group of H₃daza³⁺ is placed in an equatorial position. However, for H_xdazol^{x+} (x = 0, 1, 2), the corresponding coupling constants are significantly smaller, with a value of 5.4/1.4 Hz at pD 5.5 and 5.8/4.4 Hz at pD 10 (Fig. 2). It thus appears that in solution the hydroxy group of H_xdazol^{x+} (x = 0, 1, 2) is positioned axially. Interestingly, at a

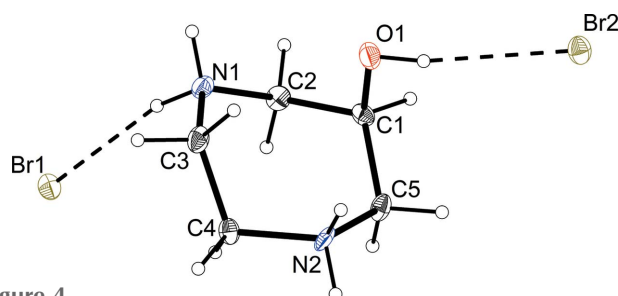


Figure 4
The molecular structure of the H₂dazol²⁺·2Br[–] unit, with the atom-numbering scheme and displacement ellipsoids drawn at the 50% probability level.

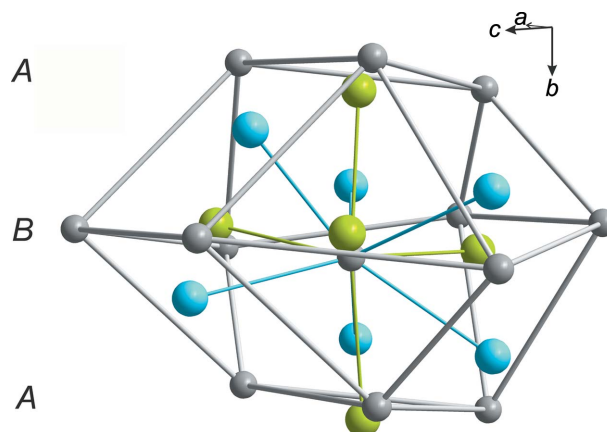


Figure 5
The distorted anticuboctahedron formed by the gravicentres of 12 H₂dazol²⁺ cations (gray spheres) together with the central H₂dazol²⁺ cation. The two crystallographically independent Br[–] anions are placed in 50% of the trigonal holes of a hexagonal layer (Br1 = green spheres) and in all of the octahedral holes (Br2 = blue spheres).

very high base concentration (5 mol l^{–1} NaOD), the signal of this proton is again shifted by about 0.2 ppm to lower frequency and appeared as a quintet with one unique coupling constant of 4.0 Hz. Obviously, the hydroxy group of dazol becomes deprotonated in such a highly alkaline medium.

In agreement with our NMR study, the H₂dazol²⁺ cation also adopted a TC conformation in the crystal structure, with the pivot atom N1 located in the isoclinal position. The puckering parameters (Boessenkool & Boeyens, 1980) of the seven-membered diazepane ring are $Q = 0.821$ (7) Å, $Q_2 = 0.506$ (7), $Q_3 = 0.647$ (7), $\varphi_2 = 86.5$ (8)° and $\varphi_3 = 92.0$ (6)°. Also, in accordance with the solution structure, the hydroxy group adopted an axial position. The different orientation of the NH₃⁺ group of H₃daza³⁺ and the OH group of H_xdazol^{x+} (x = 0, 1, 2) is remarkable. Since this difference is observed in the solid state, as well as in solution, the peculiar structure may be explained by the well-known attractive *gauche* effect (Entrena *et al.*, 1997), which proposes the preferential adoption of a *gauche* rather than a *trans* conformation for such an X–C–C–OR fragment (X = O, N).

Similar to the work performed by Liu *et al.* (1996), the crystal structure analysis presented here exhibited low precision, *i.e.* large standard uncertainties for bond angles and distances. An inspection of the displacement parameters of the C, N and O atoms indicated some significant deviations for the displacement ellipsoids from a spherical shape (Fig. 4). Considering the high conformational flexibility of the seven-membered diazepane frame, we attribute these large deviations to minor disorder rather than to thermal motion (in contrast to Liu's work, we performed data collection at –131 °C). It was, however, not possible to resolve this slight disorder in terms of a superposition of distinct individual conformers.

3.3. Supramolecular features

The cationic H₂dazol²⁺ gravicentres (dgc) are arranged into layers oriented parallel to the crystallographic *ac* plane. In

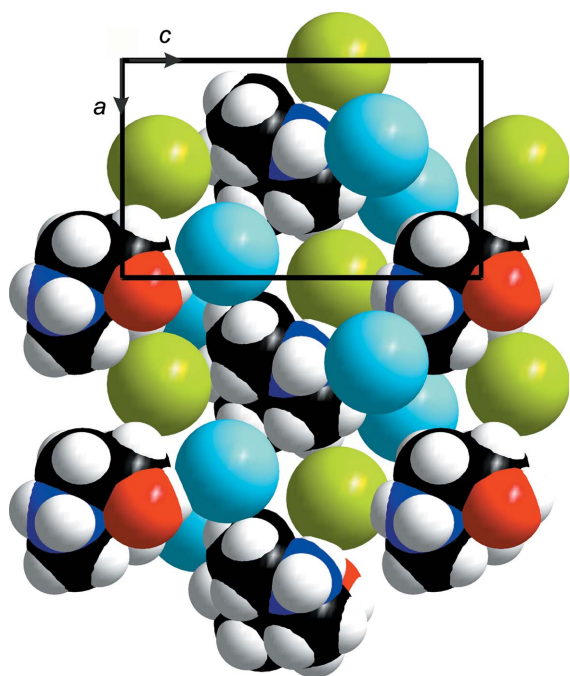


Figure 6
View of the (010) plane (space-filling model). The $\text{H}_2\text{dazol}^{2+}$ cations form a pseudo-hexagonal layer with the Br1 anions (green spheres) located in every second trigonal hole of this layer. The Br2 anions are shown as light-blue spheres and are placed in the octahedral holes above and below this layer. C, H, N and O atoms are shown as black, light-gray, dark-blue and red spheres, respectively.

these layers, each dgc is surrounded by six neighbouring dgc, forming a distorted hexagon. The layers are stacked along b in a staggered fashion ($ABABAB\dots$) and can thus be regarded as a distorted hexagonal packing. If the two adjacent layers are taken into account, each dgc receives 12 dgc neighbours, which form an anticuboctahedron (Fig. 5). However, some characteristic deviations from a regular shape are noted for this polyhedron. One reason for the distortion originates from the significant deviation of the $\text{H}_2\text{dazol}^{2+}$ cations from a spherical shape; these cations should be regarded as disks rather than spheres. Consequently, the $(\text{dgc})_{12}$ anticuboctahedron is compressed along the pseudo-hexagonal axis, as is expressed by the unequal edge lengths (5.59–7.87 Å) and short interlayer distances. Further distortion originates from the general position of the dgc and the reduced crystallographic symmetry. As a consequence, the dgc layers (and thus the equators of the anticuboctahedra) are puckered. The symmetry class of this layer group is $p12_11$ (International Tables for Crystallography, 2002; Shubnikov & Koptsik, 1974). Interestingly, the Br1 ions (green spheres in Figs. 5 and 6) are located neither in the tetrahedral nor in the octahedral holes of this packing. They are placed almost straight within the pseudo-hexagonal dgc planes. Each Br1 anion is thus surrounded by three dgc dications. Only 50% of these triangular holes are occupied. Such a packing becomes understandable if the huge difference in size between Br^- and $\text{H}_2\text{dazol}^{2+}$ is considered (Fig. 6). The entire geometry and coordination number of Br1 becomes evident if the staggered arrangement of the dgc layers is taken into account. Beside the three dgc neighbours of the triangular

Table 2
Hydrogen-bond geometry (Å, °).

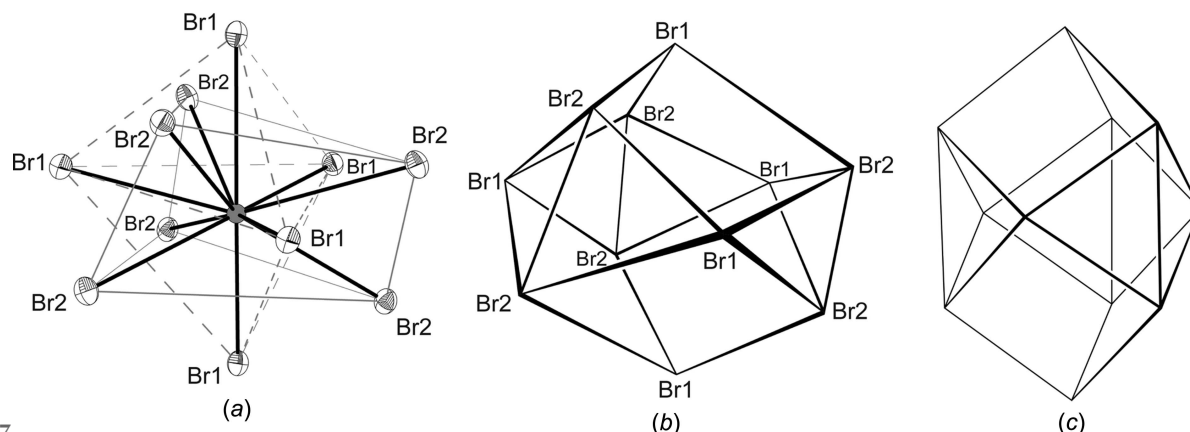
$D-H\cdots A$	$D-H$	$H\cdots A$	$D\cdots A$	$D-H\cdots A$
O1–H1O \cdots Br2	0.84 (1)	2.41 (2)	3.244 (4)	170 (8)
N1–H1N \cdots Br1	0.88 (1)	2.36 (2)	3.230 (6)	167 (7)
N1–H2N \cdots Br2 ⁱ	0.88 (1)	2.79 (6)	3.323 (6)	120 (5)
N2–H3N \cdots Br1 ⁱⁱ	0.88 (1)	2.69 (5)	3.422 (6)	142 (6)
N2–H4N \cdots Br1 ⁱⁱⁱ	0.88 (1)	2.55 (3)	3.355 (6)	153 (6)

Symmetry codes: (i) $x - \frac{1}{2}, -y + \frac{3}{2}, -z + 1$; (ii) $-x + 1, y - \frac{1}{2}, -z + \frac{1}{2}$; (iii) $-x + \frac{1}{2}, -y + 1, z + \frac{1}{2}$.

hole, the Br1 anions receive two additional dgc neighbours from adjacent dgc layers and the coordination polyhedron of Br1 can thus be described as a trigonal bipyramid. The Br2 ions (blue spheres) are located in the octahedral holes of the pseudo-hexagonal dgc packing. The coordination number of Br2 is thus six and the coordination geometry is a distorted octahedron. The $\text{H}_2\text{dazol}^{2+}$ cations, in turn, are surrounded by 11 Br anions with $\text{Br}\cdots\text{dgc}$ distances ranging from 4.0 to 6.5 Å (Fig. 7a). The resulting Br_{11} structure can be described as a distorted Edshamar polyhedron (Fig. 7b; Edshamar, 1969). Notably, the regular Edshamar polyhedron adopts D_{3h} symmetry (Fig. 7c) and is a space filler (Lidin *et al.*, 1992). Each $\text{H}_2\text{dazol}^{2+}$ entity forms N–H \cdots Br and O–H \cdots Br hydrogen bonds (Table 2). Br1 is bonded to H1N–N1, H3N–N2($-x + 1, y + \frac{1}{2}, -z + \frac{1}{2}$) and H4N–N2($-x + \frac{1}{2}, -y + 1, z - \frac{1}{2}$). Further Br1 \cdots H interactions (Br1 \cdots H2N–N1, Br1 \cdots H1–C1, Br1–H2A–C2 and Br1 \cdots H3B–C3), with Br \cdots H–N or Br \cdots H–C angles of 131–140° and Br \cdots H distances of 2.95–3.05 Å, must be regarded as very weak hydrogen bonding if they are to be regarded as hydrogen bonding at all. The sum of the van der Waals radii of Br and H is 2.95 Å (Bondi, 1964). Br2 forms only two unambiguous hydrogen bonds to H1O–O1 and H2N–N1($x + \frac{1}{2}, -y + \frac{3}{2}, -z + 1$). Again, the contacts Br2 \cdots H3A–C3, Br2 \cdots H4A–C4, Br2 \cdots H3N–N2, Br2 \cdots H2N–N1, Br2 \cdots H2B–C2, Br2 \cdots H5A–C5, Br2 \cdots H3A–C3, with Br \cdots H distances of 2.88–3.05 Å and Br \cdots H–N or Br \cdots H–C angles of 117–162° may be considered as further weak interactions which stabilize the structure. A graph-set analysis (Bernstein *et al.*, 1995) shows the hydrogen-bonding network in the $[1\bar{1}0]$ direction (Fig. 8). The Br1 and Br2 anions are μ_3 -acceptors and the N–H and O–H hydrogens are donors in three distinct ring systems, *i.e.* $R_4^7(20)$, $R_2^2(8)$ and $R_3^3(16)$. Notably, there is no direct $\text{H}_2\text{dazol}^{2+}\cdots\text{H}_2\text{dazol}^{2+}$ hydrogen bonding and, consequently, the hydroxy group of $\text{H}_2\text{dazol}^{2+}$ does not act as an acceptor. All these structural features correspond well to the packing of large charged molecular entities, as observed for instance in Zintl phases (Lidin *et al.*, 1992), and thus provide support for the ionic model.

3.4. Database survey

By studying some related literature, we became aware that the report of Liu *et al.* (1996) might not be the only example where the nature of ‘HBr’ in a crystal structure should be questioned. A search in Version 5.20 (2018) of the Cambridge Structural Database (CSD; Groom *et al.*, 2016), looking for molecular H–Br (*i.e.* for an H atom directly connected to a Br


Figure 7

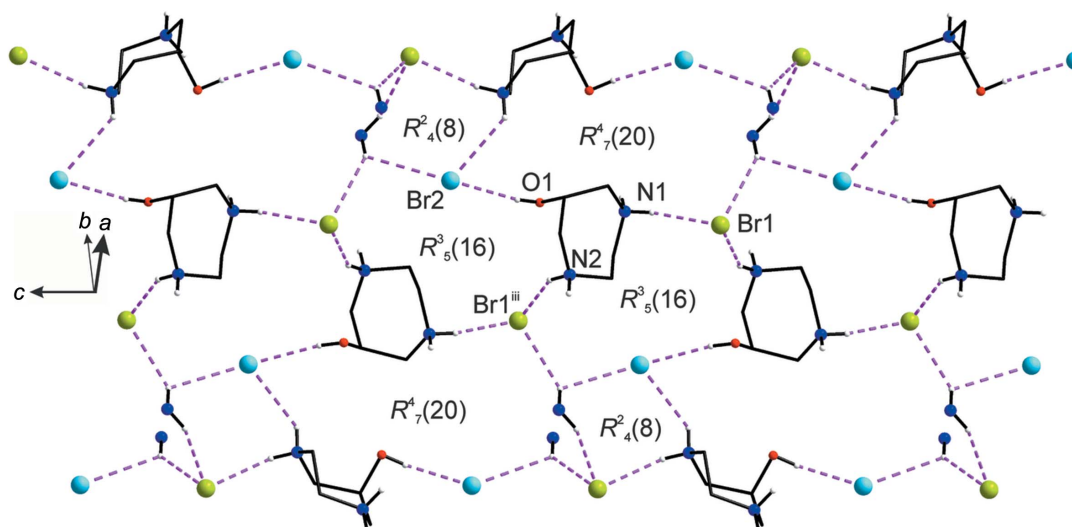
(a) The $\text{H}_2\text{dazol}^{2+}$ cation is surrounded by 11 Br^- anions. A coordination number (CN) of 11 is generated by the six Br2 anions forming a trigonal prism (tp, thin solid lines) and the five Br1 anions forming a trigonal bipyramid (tbipy, broken lines). The five vertices of the tbipy are placed over the mid-points of the five planes of the tp. (b) The observed distorted and (c) the idealized undistorted D_{3h} model (Edshammur polyhedron).

atom by a single bond), revealed a total of 69 entries (see supporting information for the full list). Some of the listed entries do not provide three-dimensional coordinates and are thus not relevant for this discussion. Furthermore, it appears that the technical term ‘hydrobromide’ may have led to confusion, since it has been used by some of the authors for a salt of a protonated organic molecule and bromide as counterion, but appeared in our search as molecular H–Br. For some of the listed compounds, the presence of HBr molecules in the structure might be quite feasible from a chemical point of view. However, there remained still a total of 13 entries [CSD refcodes BEPQIY (Růžička *et al.*, 2013), EVAMIX (Cocco *et al.*, 2004), GICSOC (Aureggi *et al.*, 2013), KEKQAS (Wang *et al.*, 1999), KONVEO (Lin *et al.*, 1990), MOMVIV (Surendra Dilip & Gowri, 2014), MOMVIV01 (Gowri *et al.*, 2015), MUFKON (Liang *et al.*, 2002), NAVFOI01 (Zhao *et al.*, 2017), NIJGOC (Liu *et al.*, 1997b), SOCZUH (Banothu *et al.*, 2014), UNESAI (Zhang & Shen, 2011) and YOTSIJ (Monte *et al.*, 1995)], where the simultaneous presence of HBr with a basic

moiety (in KEKQAS, HBr and OH^-) is proposed, with H–Br bond lengths ranging from 0.79 to 1.84 Å. It is clearly beyond the scope of this contribution to decide whether these structural assignments are correct. However, it appears that: (i) the maintainers of the database should carefully clarify whether the expression ‘hydrobromide’ refers to an ionic or rather a molecular model, and (ii) reporting such a crystal structure, authors should take the required care to clarify the bonding mode when postulating incorporation of undissociated HBr together with a basic moiety. Similar considerations might also be applicable for the so called ‘hydrochlorides’ (292 entries for a H–Cl molecule) and ‘hydroiodides’ (20 entries for a H–I molecule).

4. Conclusion

The solution and solid-state properties of the title compound do not provide evidence for a simple incorporation of HBr as intact molecules into the solid-state structure. An ionic model,


Figure 8

The hydrogen-bonding network observed for H(–N) and H(–O) H atoms as donors, and Br1 (green) and Br2 (blue) as acceptors. The plane perpendicular to the $[1\bar{1}0]$ direction is shown. The resulting cyclic structures are characterized by the descriptors $R_4^7(20)$, $R_4^4(8)$ and $R_5^3(16)$. [Symmetry code: (iii) $-x + \frac{1}{2}, -y + 1, z + \frac{1}{2}$]

comprising one $\text{H}_2\text{dazol}^{2+}$ cation and two Br^- anions is clearly a better explanation. According to the structure postulated by Liu *et al.* (1996), the two HBr molecules would not be bonded to other moieties by strong interactions (such as Coulombic forces or hydrogen bonding). The $(\text{Br}1 -)\text{H} \cdots \text{H}(-\text{Br}2)$ separation of 2.24 Å roughly corresponds to the sum of the van der Waals radii of two H atoms (2.20 Å; Bondi, 1964) and, as a consequence, the two HBr molecules would not act as H-atom donors in hydrogen bonds. One could thus expect that liberation of HBr should occur readily even at moderate temperatures.

For further clarification of this question, we grew single crystals of the title compound and repeated the X-ray analysis. We have shown that it is possible to refine the crystal structure in terms of an ordinary ammonium salt (see §2.2, *Refinement*). There is thus no need to postulate the rather exotic incorporation of molecular HBr into the crystal structure. We think that, in such a case, it is more advisable to choose the model which also directly explains the observed chemical properties (acid–base behaviour and breakdown of the structure upon HBr elimination above 300 °C).

Acknowledgements

We thank Dr Volker Huch for the measurement of the data set. Funding for this research was provided by Universität des Saarlandes.

References

- Aureggi, V., Ehmke, V., Wieland, J., Schweizer, W. B., Bernet, B., Bur, D., Meyer, S., Rottmann, M., Freymond, C., Brun, R., Breit, B. & Diederich, F. (2013). *Chem. Eur. J.* **19**, 155–164.
- Banothu, J., Khanapur, M., Basavoju, S., Bavantula, R., Narra, M. & Abbagani, S. (2014). *RSC Adv.* **4**, 22866–22874.
- Bernstein, J., Davis, R. E., Shimon, L. & Chang, N.-L. (1995). *Angew. Chem. Int. Ed. Engl.* **34**, 1555–1573.
- Boessenkool, I. K. & Boeyens, J. C. A. (1980). *J. Cryst. Mol. Struct.* **10**, 11–18.
- Bondi, A. (1964). *J. Phys. Chem.* **68**, 441–451.
- Brandenburg, K. (2007). *DIAMOND*. Crystal Impact GbR, Bonn, Germany.
- Bruker (2010). *APEX* and *SAINT*. Bruker AXS Inc., Madison, Wisconsin, USA.
- Cocco, M. T., Congiu, C., Onnis, V. & Ianelli, S. (2004). *Heterocycles*, **63**, 259–270.
- Edshammar, L.-E. (1969). PhD thesis, University of Stockholm, Sweden.
- Eliel, E. L., Allinger, N. L., Angyal, S. J. & Morrison, G. A. (1965). In *Conformational Analysis*. New York: Interscience Publishers–John Wiley.
- Entrena, A., Campos, J., Gomez, J. A., Gallo, M. A. & Espinosa, A. (1997). *J. Org. Chem.* **62**, 337–349.
- Glusker, J. P., Lewis, M. & Rossi, M. (1994). In *Crystal Structure Analysis for Chemists and Biologists*. Weinheim: VCH Publishers.
- Gowri, S., Uma Devi, T., Priya, S., Surendra Dilip, C., Selvanayagam, S. & Lawrence, N. (2015). *Spectrochim. Acta Part A*, **143**, 192–199.
- Groom, C. R., Bruno, I. J., Lightfoot, M. P. & Ward, S. C. (2016). *Acta Cryst.* **B72**, 171–179.
- International Tables for Crystallography (2002). Vol. E, *Subperiodic Groups*, edited by V. Kopsky & D. B. Litvin. Chester: International Union of Crystallography, and Dordrecht: Kluwer Academic Publishers.
- Ivanov, I. L., Mazurin, M. O., Tsvetkov, D. S., Malyshev, D. A., Sereda, V. V. & Zuev, A. Y. (2019). *Thermochim. Acta*, **674**, 58–62.
- Krause, L., Herbst-Irmer, R., Sheldrick, G. M. & Stalke, D. (2015). *J. Appl. Cryst.* **48**, 3–10.
- Liang, F., Li, Y.-Z., Wu, C.-T. & Liu, S.-M. (2002). *Acta Cryst.* **E58**, m950–m952.
- Lidin, S., Popp, T., Somer, M. & Schnering, H. G. (1992). *Angew. Chem. Int. Ed. Engl.* **31**, 924–927.
- Lin, L.-Z., Cordell, G. A., Ni, C.-Z. & Clardy, J. (1990). *Phytochemistry*, **29**, 965–968.
- Liu, S.-H., Xue, G.-P., Zhang, Z.-H., Fu, E.-Q., Wu, C.-T. & Yang, Q.-C. (1997a). *Chin. J. Struct. Chem.* **16**, 355–357.
- Liu, Y., Xue, G.-P., Wu, C.-T., Luo, B.-S. & Chen, L.-R. (1996). *Chin. J. Struct. Chem.* **15**, 371–373.
- Liu, Y., Xue, G.-P., Wu, C.-T., Luo, B.-S. & Chen, L.-R. (1997b). *Chin. J. Struct. Chem.* **16**, 338–341.
- Longuet-Higgins, H. C. (2002). *Mol. Phys.* **100**, 11–20.
- Martincigh, B. S. & Marsicano, F. (1995). *J. Coord. Chem.* **34**, 365–381.
- Monte, A. P., Marona-Lewicka, D., Kanthasamy, A., Sanders-Bush, E. & Nichols, D. E. (1995). *J. Med. Chem.* **38**, 958–966.
- Müller, P., Herbst-Irmer, R., Spek, A. L., Schneider, T. R. & Sawaya, M. R. (2006). *Crystal Structure Refinement – A Crystallographer's Guide to SHELXL*. Oxford University Press.
- Neis, C., Petry, D., Demangeon, A., Morgenstern, B., Kuppert, D., Huppert, J., Stucky, S. & Hegetschweiler, K. (2010). *Inorg. Chem.* **49**, 10092–10107.
- NIST (2019). *Standard Reference Database*, Number 69, edited by P. J. Linstrom & W. G. Mallard. National Institute of Standards and Technology, Gaithersburg MD, 20899, <https://doi.org/10.18434/T4D303> (retrieved February 27, 2019).
- Parsons, S., Flack, H. D. & Wagner, T. (2013). *Acta Cryst.* **B69**, 249–259.
- Romba, J., Kuppert, D., Morgenstern, B., Neis, C., Steinhauser, S., Weyhermüller, T. & Hegetschweiler, K. (2006). *Eur. J. Inorg. Chem.* pp. 314–328.
- Růžička, A., Padělková, Z., Švec, P., Pejchal, V., Česlová, L. & Holeček, J. (2013). *J. Organomet. Chem.* **732**, 47–57.
- Saari, W. S., Raab, A. W. & King, S. W. (1971). *J. Org. Chem.* **36**, 1711–1714.
- Sheldrick, G. M. (2015a). *Acta Cryst.* **A71**, 3–8.
- Sheldrick, G. M. (2015b). *Acta Cryst.* **C71**, 3–8.
- Shubnikov, A. V. & Koptsik, V. A. (1974). In *Symmetry in Science and Art*. New York: Plenum Press.
- Spek, A. L. (2009). *Acta Cryst.* **D65**, 148–155.
- Surendra Dilip, C. & Gowri, S. (2014). *CSD Communication* (refcode MOMVIV). CCDC, Cambridge, England.
- Wang, H. M. J., Chen, C. Y. L. & Lin, I. J. B. (1999). *Organometallics*, **18**, 1216–1223.
- Zhang, F. L. & Shen, L. (2011). *CSD Communication* (deposition number 737932). CCDC, Cambridge, England.
- Zhao, W., Wang, Y. & Wang, A. (2017). *J. Mater. Sci. Chem. Eng.* **5**, 1–11.

supporting information

Acta Cryst. (2019). C75, 678-685 [https://doi.org/10.1107/S2053229619005321]

HBr or not HBr? That is the question: crystal structure of 6-hydroxy-1,4-diazepane-1,4-dium dibromide redetermined

Mateusz Piontek, Bernd Morgenstern, Nils Steinbrück, Bastian Oberhausen, Guido Kickelbick and Kaspar Hegetschweiler

Computing details

Data collection: *APEX2* (Bruker, 2010); cell refinement: *SAINTE* (Bruker, 2010); data reduction: *SAINTE* (Bruker, 2010); program(s) used to solve structure: *SHELXT2014* (Sheldrick, 2015a); program(s) used to refine structure: *SHELXL2014* (Sheldrick, 2015b); molecular graphics: *DIAMOND* (Brandenburg, 2007); software used to prepare material for publication: *PLATON* (Spek, 2009).

6-Hydroxy-1,4-diazepane-1,4-dium dibromide

Crystal data

$C_5H_{14}N_2O^{2+} \cdot 2Br^-$

$M_r = 278.00$

Orthorhombic, $P2_12_12_1$

$a = 7.7005$ (4) Å

$b = 9.2774$ (5) Å

$c = 12.6853$ (6) Å

$V = 906.25$ (8) Å³

$Z = 4$

$F(000) = 544$

$D_x = 2.038$ Mg m⁻³

Mo $K\alpha$ radiation, $\lambda = 0.71073$ Å

Cell parameters from 1133 reflections

$\theta = 3.8$ – 25.7°

$\mu = 8.89$ mm⁻¹

$T = 142$ K

Needle, colourless

$0.23 \times 0.07 \times 0.02$ mm

Data collection

Bruker APEXII CCD

diffractometer

Radiation source: sealed tube

φ and ω scans

Absorption correction: multi-scan

(SADABS; Krause *et al.*, 2015)

$T_{\min} = 0.576$, $T_{\max} = 0.746$

4858 measured reflections

2089 independent reflections

1789 reflections with $I > 2\sigma(I)$

$R_{\text{int}} = 0.050$

$\theta_{\max} = 27.6^\circ$, $\theta_{\min} = 2.7^\circ$

$h = -8 \rightarrow 10$

$k = -10 \rightarrow 12$

$l = -16 \rightarrow 15$

Refinement

Refinement on F^2

Least-squares matrix: full

$R[F^2 > 2\sigma(F^2)] = 0.037$

$wR(F^2) = 0.063$

$S = 0.93$

2089 reflections

106 parameters

5 restraints

Primary atom site location: structure-invariant direct methods

Secondary atom site location: difference Fourier map

Hydrogen site location: mixed

H atoms treated by a mixture of independent and constrained refinement

$w = 1/[\sigma^2(F_o^2)]$

where $P = (F_o^2 + 2F_c^2)/3$

$$(\Delta/\sigma)_{\max} < 0.001$$

$$\Delta\rho_{\max} = 0.61 \text{ e } \text{\AA}^{-3}$$

$$\Delta\rho_{\min} = -0.51 \text{ e } \text{\AA}^{-3}$$

Absolute structure: Flack x determined using
646 quotients [(I+)-(I-)]/[(I+)+(I-)] (Parsons *et al.*, 2013)
Absolute structure parameter: 0.05 (2)

Special details

Geometry. All esds (except the esd in the dihedral angle between two l.s. planes) are estimated using the full covariance matrix. The cell esds are taken into account individually in the estimation of esds in distances, angles and torsion angles; correlations between esds in cell parameters are only used when they are defined by crystal symmetry. An approximate (isotropic) treatment of cell esds is used for estimating esds involving l.s. planes.

Fractional atomic coordinates and isotropic or equivalent isotropic displacement parameters (\AA^2)

	x	y	z	$U_{\text{iso}}^*/U_{\text{eq}}$
C1	0.5844 (9)	0.5995 (7)	0.5028 (5)	0.0123 (15)
H1	0.6966	0.6299	0.5357	0.015*
C2	0.5905 (8)	0.6493 (8)	0.3890 (5)	0.0133 (15)
H2A	0.6493	0.7441	0.3860	0.016*
H2B	0.6615	0.5803	0.3479	0.016*
C3	0.2761 (9)	0.5574 (9)	0.3664 (5)	0.0152 (16)
H3A	0.1864	0.5590	0.3106	0.018*
H3B	0.2205	0.5892	0.4329	0.018*
C4	0.3390 (9)	0.4052 (8)	0.3801 (5)	0.0144 (17)
H4A	0.2443	0.3376	0.3617	0.017*
H4B	0.4370	0.3874	0.3313	0.017*
C5	0.5688 (8)	0.4385 (8)	0.5208 (5)	0.0139 (16)
H5A	0.6604	0.3890	0.4797	0.017*
H5B	0.5902	0.4181	0.5963	0.017*
N1	0.4167 (7)	0.6626 (8)	0.3381 (4)	0.0133 (13)
H1N	0.433 (8)	0.645 (8)	0.2703 (17)	0.016*
H2N	0.382 (9)	0.753 (3)	0.340 (5)	0.016*
N2	0.3970 (9)	0.3769 (6)	0.4909 (5)	0.0139 (14)
H3N	0.403 (10)	0.2828 (18)	0.498 (6)	0.017*
H4N	0.321 (7)	0.410 (7)	0.537 (4)	0.017*
O1	0.4508 (6)	0.6777 (6)	0.5558 (3)	0.0180 (12)
H1O	0.491 (9)	0.661 (9)	0.616 (3)	0.027*
Br1	0.48660 (9)	0.54448 (8)	0.10235 (5)	0.01472 (18)
Br2	0.61165 (9)	0.65666 (9)	0.79166 (5)	0.01602 (18)

Atomic displacement parameters (\AA^2)

	U^{11}	U^{22}	U^{33}	U^{12}	U^{13}	U^{23}
C1	0.010 (4)	0.012 (4)	0.014 (3)	-0.003 (3)	-0.002 (3)	-0.002 (3)
C2	0.009 (3)	0.014 (4)	0.017 (3)	-0.003 (3)	0.000 (3)	0.002 (4)
C3	0.017 (4)	0.018 (4)	0.010 (3)	0.002 (4)	0.001 (3)	0.003 (4)
C4	0.010 (4)	0.017 (4)	0.016 (4)	-0.001 (3)	-0.006 (3)	-0.001 (3)
C5	0.010 (3)	0.017 (4)	0.014 (3)	-0.001 (3)	-0.003 (3)	0.005 (3)
N1	0.016 (3)	0.013 (3)	0.011 (3)	0.003 (3)	0.001 (2)	0.002 (3)
N2	0.014 (3)	0.014 (4)	0.013 (3)	0.006 (3)	-0.003 (2)	0.005 (3)

O1	0.019 (3)	0.021 (3)	0.013 (2)	0.007 (3)	-0.004 (2)	-0.005 (2)
Br1	0.0136 (3)	0.0172 (4)	0.0134 (3)	0.0003 (3)	-0.0008 (3)	-0.0018 (3)
Br2	0.0166 (4)	0.0195 (4)	0.0120 (3)	-0.0024 (4)	0.0007 (3)	0.0008 (4)

Geometric parameters (Å, °)

C1—O1	1.427 (8)	C4—N2	1.498 (8)
C1—C5	1.516 (10)	C4—H4A	0.9900
C1—C2	1.517 (9)	C4—H4B	0.9900
C1—H1	1.0000	C5—N2	1.490 (9)
C2—N1	1.491 (8)	C5—H5A	0.9900
C2—H2A	0.9900	C5—H5B	0.9900
C2—H2B	0.9900	N1—H1N	0.883 (13)
C3—N1	1.502 (9)	N1—H2N	0.882 (13)
C3—C4	1.503 (10)	N2—H3N	0.879 (13)
C3—H3A	0.9900	N2—H4N	0.884 (13)
C3—H3B	0.9900	O1—H1O	0.839 (13)
O1—C1—C5	111.9 (6)	C3—C4—H4B	109.3
O1—C1—C2	108.4 (5)	H4A—C4—H4B	107.9
C5—C1—C2	116.5 (6)	N2—C5—C1	114.2 (6)
O1—C1—H1	106.5	N2—C5—H5A	108.7
C5—C1—H1	106.5	C1—C5—H5A	108.7
C2—C1—H1	106.5	N2—C5—H5B	108.7
N1—C2—C1	114.2 (5)	C1—C5—H5B	108.7
N1—C2—H2A	108.7	H5A—C5—H5B	107.6
C1—C2—H2A	108.7	C2—N1—C3	119.3 (6)
N1—C2—H2B	108.7	C2—N1—H1N	106 (4)
C1—C2—H2B	108.7	C3—N1—H1N	103 (5)
H2A—C2—H2B	107.6	C2—N1—H2N	110 (5)
N1—C3—C4	113.9 (6)	C3—N1—H2N	113 (5)
N1—C3—H3A	108.8	H1N—N1—H2N	104 (7)
C4—C3—H3A	108.8	C5—N2—C4	115.9 (6)
N1—C3—H3B	108.8	C5—N2—H3N	108 (5)
C4—C3—H3B	108.8	C4—N2—H3N	107 (5)
H3A—C3—H3B	107.7	C5—N2—H4N	106 (5)
N2—C4—C3	111.7 (6)	C4—N2—H4N	111 (4)
N2—C4—H4A	109.3	H3N—N2—H4N	109 (7)
C3—C4—H4A	109.3	C1—O1—H1O	94 (5)
N2—C4—H4B	109.3		
O1—C1—C2—N1	-44.8 (8)	C1—C2—N1—C3	-35.3 (9)
C5—C1—C2—N1	82.5 (8)	C4—C3—N1—C2	-39.4 (8)
N1—C3—C4—N2	88.3 (7)	C1—C5—N2—C4	55.1 (8)
O1—C1—C5—N2	55.6 (8)	C3—C4—N2—C5	-75.7 (7)
C2—C1—C5—N2	-69.9 (8)		

Hydrogen-bond geometry (Å, °)

<i>D</i> —H··· <i>A</i>	<i>D</i> —H	H··· <i>A</i>	<i>D</i> ··· <i>A</i>	<i>D</i> —H··· <i>A</i>
O1—H1O···Br2	0.84 (1)	2.41 (2)	3.244 (4)	170 (8)
N1—H1N···Br1	0.88 (1)	2.36 (2)	3.230 (6)	167 (7)
N1—H2N···Br2 ⁱ	0.88 (1)	2.79 (6)	3.323 (6)	120 (5)
N2—H3N···Br1 ⁱⁱ	0.88 (1)	2.69 (5)	3.422 (6)	142 (6)
N2—H4N···Br1 ⁱⁱⁱ	0.88 (1)	2.55 (3)	3.355 (6)	153 (6)

Symmetry codes: (i) $x-1/2, -y+3/2, -z+1$; (ii) $-x+1, y-1/2, -z+1/2$; (iii) $-x+1/2, -y+1, z+1/2$.